R10

Identifying the Sources of Random Telegraph Noises in Pixels of CMOS Image Sensors

Calvin Yi-Ping Chao[1], Meng-Hsu Wu[1], Shang-Fu Yeh[1], Kuo-Yu Chou[1], Honyih Tu[1], Chi-Lin Lee[1], Yin Chin[1], Philippe Paillet[2], and Vincent Goiffon[3]

[1]Taiwan Semiconductor Manufacturing Company, Hsinchu, Taiwan, ROC
Tel: (886) 3-5636688 ext 703-8243, email: calvin_chao@tsmc.com
[2]CEA, DAM, DIF, F-91297 Arpajon, France
[3]ISAE-SUPAERO, Université de Toulouse, 31055 Toulouse, France

INTRODUCTION

It is well reported in literature that the pixels on the distribution tail of the dark random noises (RN) often show the characteristic behavior of the random telegraph signals (RTS) [1-5]. Such noises are called the random telegraph noises (RTN) and the pixels with RTN are referred to as the RTN pixels. The magnitude of the RTN in worst cases can be 10 to 100 times higher than the median or the average RN for a large array. An important but less studied topic is that there are many different types of RTN which might be originated from different locations of the pixels and due to different physical mechanisms.

In this paper, we present the identification of different RTN sources in CIS before and after X-ray irradiation. The X-ray is used as a tool to alter the RTN composition, hopefully shedding some light on the process-induced damage (PID) in CIS fabrication.

EXPERIMENTS AND KEY FINDINGS

The test chip is an 8.3MP, 1.1µm pixel, stacked CIS. The pixel layer is fabricated in a 45 nm BSI technology; the ASIC layer in a 65 nm low-power mixed-mode process. The chip architecture, operation voltages, control timing, and key performance parameters were reported in [2-5]. In particular, we have confirmed in [2-5] that the circuit performance was not degraded by X-ray up to 2 Mrad(SiO_2) total ionizing dose (TID). Therefore, the observed changes of RN and RTN composition due to X-ray irradiation can be attributed exclusively to the pixels.

Specifically, we find that the RN of the noisiest pixels can be classified into the following 4 categories: (1) the dark signal (DS) shot noise; (2) the source follower (SF) MOSFET channel RTN; (3) the RTN due to the variable transfer-gate-induced sense node (SN) leakage [5]; and (4) the RTN due to the variable photodiode dark current (DC). For convenience, the last 3 RTN types are referred to as the SF-RTN, the GIDL-RTN, and the DC-RTN, respectively. Both of the GIDL-RTN and the DC-RTN are caused by the variable junction leakage (VJL) [1].

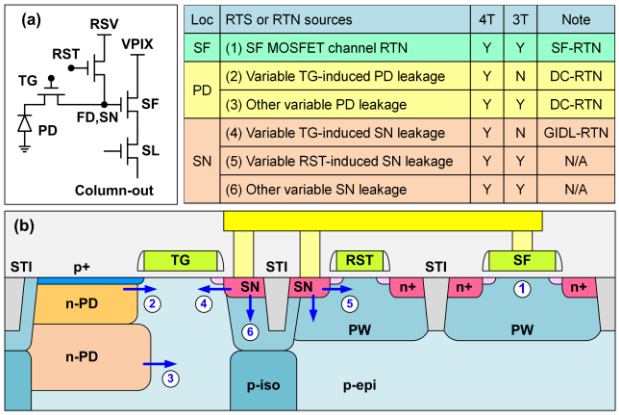

Loc	RTS or RTN sources	4T	3T	Note
SF	(1) SF MOSFET channel RTN	Y	Y	SF-RTN
PD	(2) Variable TG-induced PD leakage	Y	N	DC-RTN
	(3) Other variable PD leakage	Y	Y	DC-RTN
SN	(4) Variable TG-induced SN leakage	Y	N	GIDL-RTN
	(5) Variable RST-induced SN leakage	Y	Y	N/A
	(6) Other variable SN leakage	Y	Y	N/A

Figure 1. (a) A generic 4T pinned photodiode (PPD) pixel. (b) The potential locations and types of RTNs in the pixel.

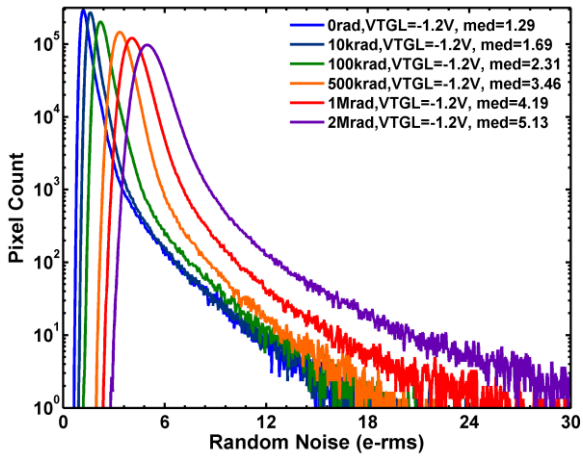

Figure 2. The random noise histograms before and after X-ray irradiation with various TID up to 2 Mrad(SiO_2).

Fig. 1 shows a generic 4T pixel schematic and the conceptual classification of the RTN according to their locations, e.g., the SF, the SN, and the PD; and the types, e.g., the MOSFET channel RTN, the RTN caused by VJL related to the gate-induced drain leakage (GIDL) or not related to GIDL. In this work, the observed RTN types are item (1), (3), and (4) in Fig. 1(b); we did not find evidence

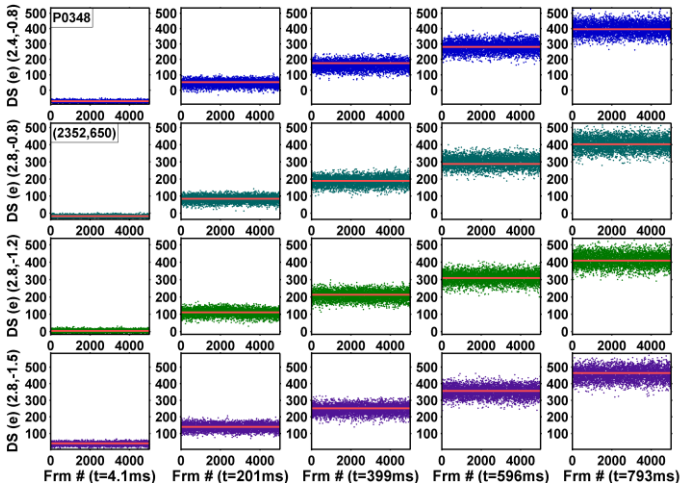

Figure 3. An example pixel with dark-signal shot noise.

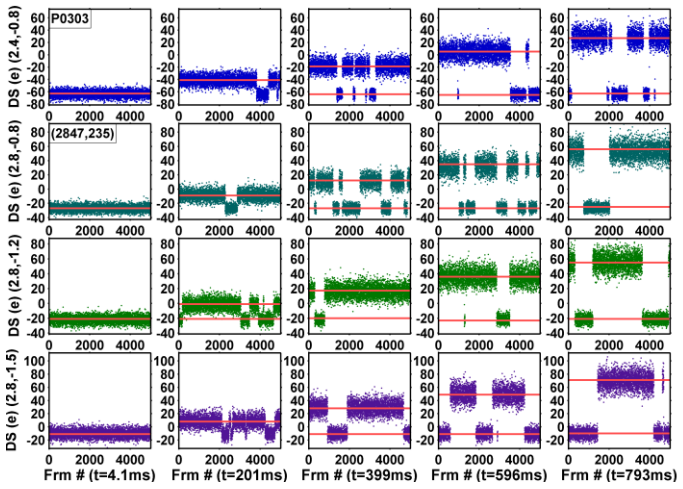

Figure 4. An example pixel with DC-RTN.

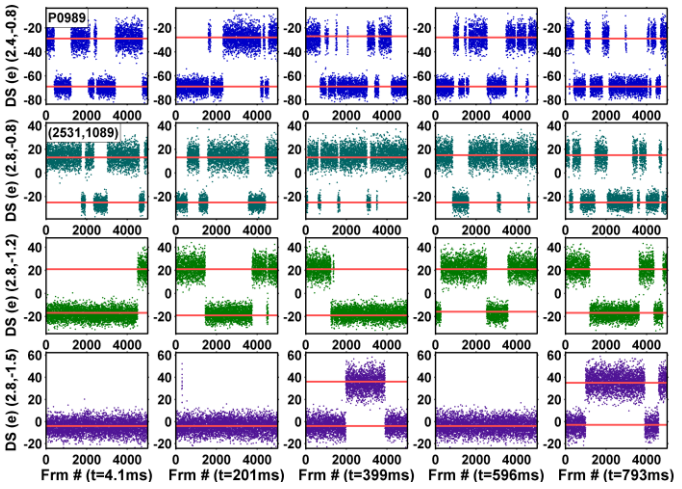

Figure 5. An example pixel with GIDL-RTN.

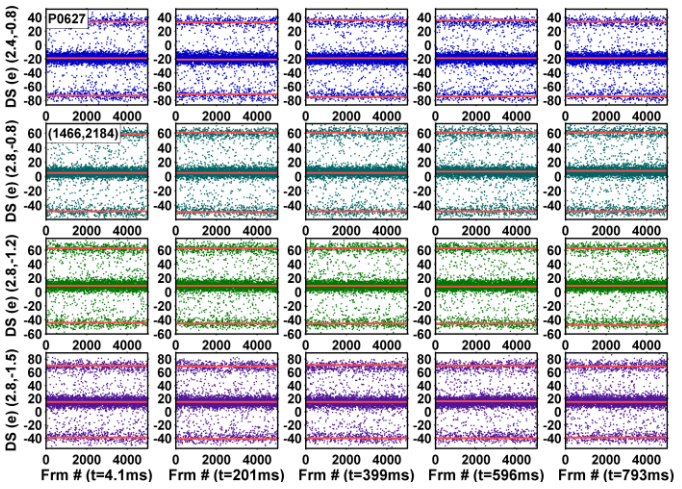

Figure 6. An example pixel with SF-RTN.

of item (2). The observation the reset-gate GIDL-RTN, item (5), on a non-CIS chip is reported separately in [6].

Fig. 2 shows the RN histograms of chips exposed to various X-ray TIDs, from 0 to 2 Mrad(SiO_2). Clearly, there is a systematic increase of RN in the main population dominated by the thermal and flicker noises, and the RN long tail dominated by RTN, as the TID increases.

RN AND RTN WAVEFORMS

The primary method to identify the sources of RN and RTN is to examine the dark signal waveforms of individual pixels and their dependence on the PD integration time, the SN charge retention time, the reset-drain ON-voltage RSVH, and the transfer-gate OFF-voltage VTGL. The SN charge retention time is the time for correlated double sampling (CDS) in the global ADC architecture used for this chip. It would include the AD conversion time as well in a column-parallel ADC architecture.

In our previous study [5], the RN was measured under a special test mode such that the TG was disabled during the CDS operation. There was no charge transfer from PD to SN; therefore, there was no RN contribution from DC-RTN or DS shot noise. Only the SF-RTN and the SN GIDL-RTN were observed. However, in this work the RN was measured under the normal operation mode such that TG was enabled during CDS.

Figs. 3-6 are the 5,000-frame dark signal waveforms for 4 example pixels, measured under 20 conditions. The 4-by-5 combo plots for each pixel represent 5 different integration times, from 4.1 ms to 793 ms, along the horizontal direction, and 4 different operation voltages, (RSTV, VTGL) = (2.8V, –1.5V), (2.8V, –1.2V), (2.8V, –0.8V), (2.4V, –0.8V), along the vertical direction.

Both of the DS shot noise in Fig. 3 and the DC-RTN in Fig. 4 show a linear dependence on integration time and a weak dependence on (RSTV, VTGL). The waveforms of the GIDL-RTN in Fig. 5 depend strongly on (RSTV, VTGL), but are almost independent of integration time. In contrast, the SF-RTN magnitudes in Fig. 6 are neither dependent on (RSTV, VTGL), nor on integration time.

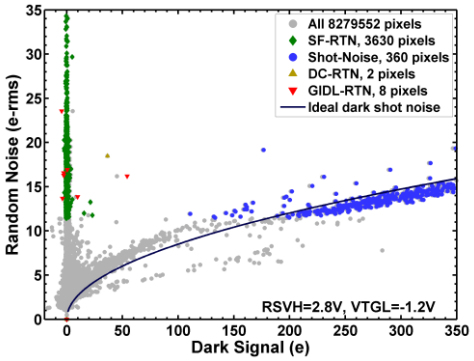

Figure 7(a). Chip not irradiated by X-ray, (RSTV, VTGL) = (2.8V, –1.2V).

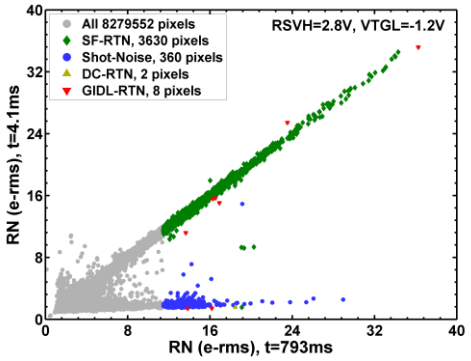

Figure 8(a). Chip not irradiated by X-ray, (RSTV, VTGL) = (2.8V, –1.2V).

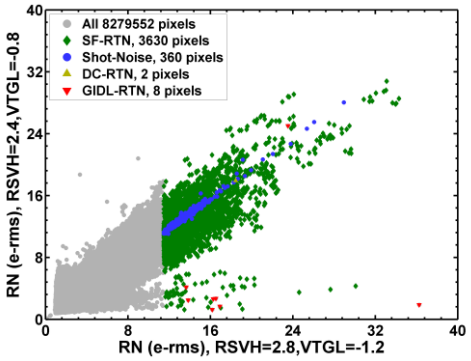

Figure 9(a). No X-ray, 4,000 noisiest pixels selected from the (2.8V, –1.2V) data.

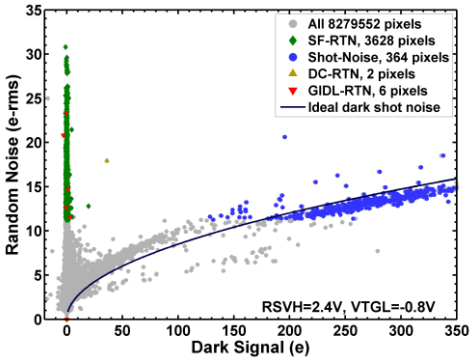

Figure 7(b). Chip not irradiated by X-ray, (RSTV, VTGL) = (2.4V, –0.8V).

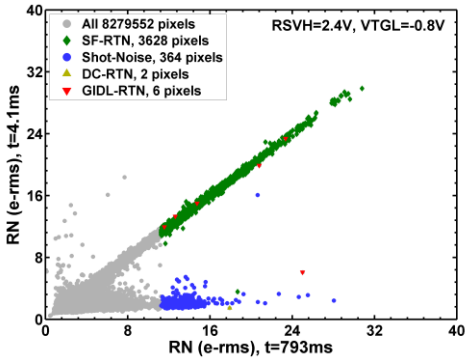

Figure 8(b). Chip not irradiated by X-ray, (RSTV, VTGL) = (2.4V, –0.8V).

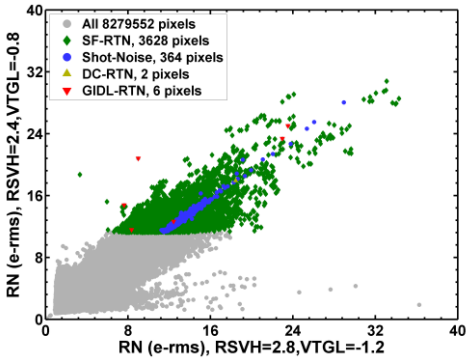

Figure 9(b). No X-ray, 4,000 noisiest pixels selected from the (2.4V, –0.8V) data.

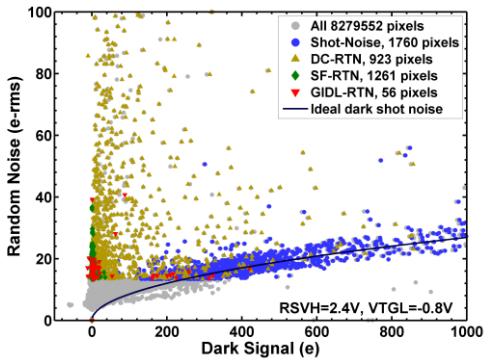

Figure 7(c). Chip irradiated by 1 Mrad X-ray, (RSTV, VTGL) = (2.8V, –1.2V).

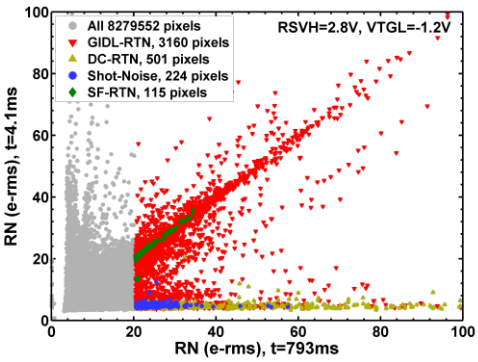

Figure 8(c). Chip irradiated by 1 Mrad X-ray, (RSTV, VTGL) = (2.8V, –1.2V).

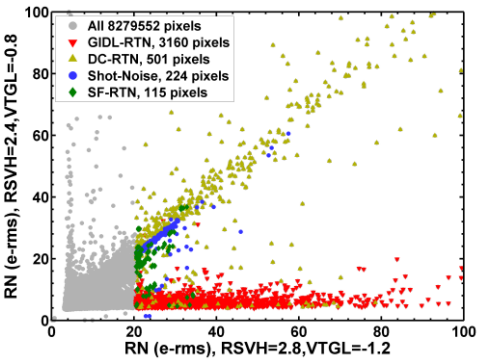

Figure 9(c). 1 Mrad X-ray, 4,000 noisiest pixels selected from the (2.8V, –1.2V) data.

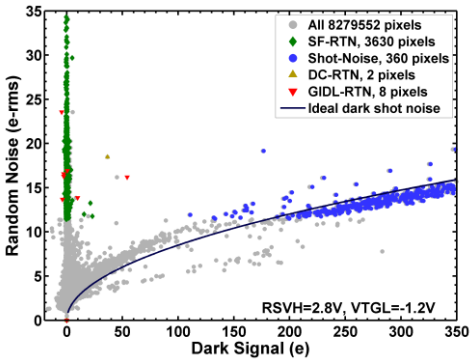

Figure 7(d). Chip irradiated by 1 Mrad X-ray, (RSTV, VTGL) = (2.4V, –0.8V).

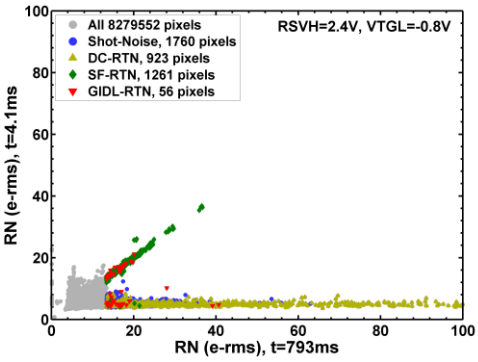

Figure 8(d). Chip irradiated by 1 Mrad X-ray, (RSTV, VTGL) = (2.4V, –0.8V).

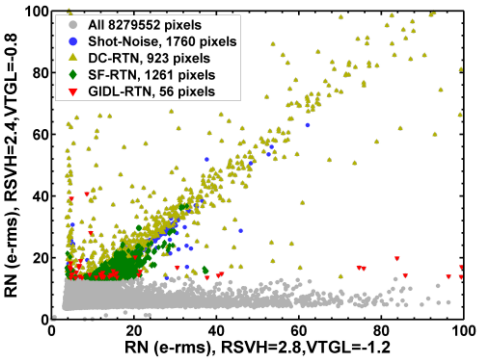

Figure 9(d). 1 Mrad X-ray, 4,000 noisiest pixels selected from the (2.4V, –0.8V) data.

Furthermore, it was reported in [5] that the GIDL-RTN depended linearly on the SN charge retention time, while the SF-RTN did not.

IDENTIFYING THE RN AND RTN TYPES

The behaviors of different RN and RTN types can be further illustrated by the correlation between the RN and the integration time in Fig. 7, the correlation between the RN of a short integration time (4.1 ms) and the RN of a long integration time (793 ms) in Fig. 8, and the RN under a GIDL-reduced bias (RSTV, VTGL) = (2.4V, –0.8V) and the RN under a standard bias (2.8V, –1.2V) in Fig. 9. For each of the comparison, we focus on the 4,000 noisiest pixels from the 1 Mrad irradiated chip and the chip not exposed to X-ray, measured under the GIDL-reduced and the standard biases. Thus, each of Figs. 7-9 consists of 4 sub figures, (a), (b), (c), and (d).

The 4,000 noisiest pixels are sorted into 4 groups: DS shot noise, DC-RTN, GIDL-RTN, and SF-RTN, labeled by different symbols accordingly. The sorting was performed semi-automatically, first by software, then, double checked by visual inspection on the DS waveforms described in the previous section. The entire 8.3M pixels are plotted as the grey dots in the background for reference.

The key observations are discussed below. Without X-ray damage, Figs. 7(a)-(b) show that the SF-RTN is dominant among the noisiest pixels. Almost all SF-RTN pixels show small dark signals. Some pixels with very large dark signals show the shot noise characteristics clearly. They follow the well-known Poisson statistics, $RN \propto \sqrt{DS}$. These DS shot noises are typically smaller than the SF-RTN magnitudes. There are very few pixels showing DC-RTN or GIDL-RTN. The noise composition remains the same under different bias conditions.

In contrast, after X-ray irradiation, Figs. 7(c)-(d) show that the numbers of DC-RTN, GIDL-RTN, and DS shot noise pixels are significantly increased. Under the standard bias, the GIDL-RTN pixels clearly dominate. The number of GIDL-RTN pixels dramatically decreases under the GIDL-reduced bias, surpassed by the SF-RTN and DC-RTN. It is interesting to point out that pixels with high DC-RTN do not necessarily have high DC or DS.

Next, we examine the RN dependence on integration time. Without X-ray, Figs. 8(a)-(b) show that the SF-RTN and DS shot noise pixels are separated distinctly into 2 branches. The SF-RTN pixels are located along the diagonal line, showing no dependence on integration time. While DS shot noise pixels on the lower branch show linear dependence on integration time.

After X-ray irradiation, as shown in Figs 8(c)-(d), the dominant GIDL-RTN is independent of the integration time, while the DC-RTN is obviously dependent on integration time. It is additionally reported in [5] that the GIDL-RTN depends linearly on the SN charge retention time, while SF-RTN does not.

Figs. 9(a)-(d) compare the RN correlation between the GIDL-reduced bias and the standard bias, with and without X-ray irradiation. For chips not exposed to X-ray, as in Figs. 9(a)-(b), the RTN is primarily SF-RTN, relatively insensitive to bias.

After X-ray irradiation, the magnitudes of highest noises are increased due to the generation of many GIDL-RTN and DC-RTN pixels. Note that different scales of the X and Y axes are used in Fig. 9(a)-(b) and 9(c)-(d). Again, Figs. 9(c)-(d) show that the GIDL-RTN pixels dominate under the normal bias, but are almost completely suppressed under the GIDL-reduced bias.

CONCLUSION

Finally, we summarize the noise compositions of the 4,000 noisiest pixels for the 4 cases discussed above into a bar chart Fig. 10 to highlight the changes resulted from X-ray irradiation and the effects of bias conditions. The main findings of this study are that for the CIS before X-ray irradiation, the dominant RTN type is the SF-RTN. Very few pixels show DC-RTN or GIDL-RTN. In contrast, for the chip exposed to 1 Mrad X-ray, a dramatic increase of DS shot noise, DC-RTN, and GIDL-RTN is observed. Under the standard bias, RSVH = 2.8V, VTGL = –1.2V, the GIDL-RTN dominates; while under the GIDL-reduced bias, RSVH = 2.4V, VTGL = –0.8V, the DC-RTN becomes dominant and the GIDL-RTN is significantly suppressed.

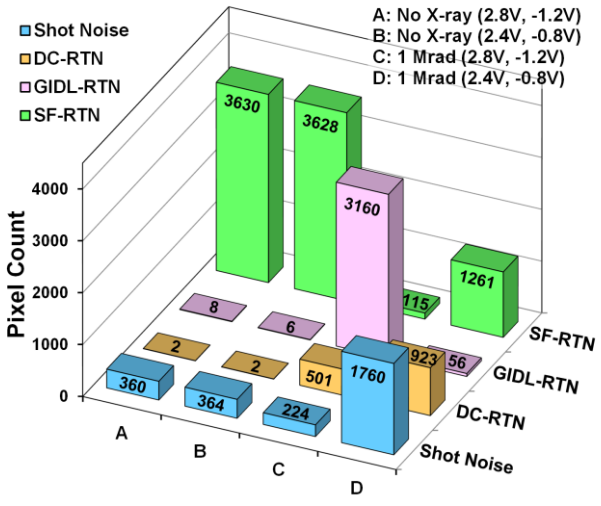

Figure 10. Composition of RN/RTN of 4,000 noisiest pixels.

Reference

[1] E. Simoen and C. Claeys, Random Telegraph Signals in Semiconductor Devices. Bristol, UK: IOP Publishing, 2016.
[2] C. Y.-P. Chao *et al.*, J-EDS, vol. 5, pp. 79–89, 2017.
[3] C. Y.-P. Chao *et al.*, IISW 2017, pp. 35–38.
[4] C. Y.-P. Chao *et al.*, Sensors 17, no. 2, 2017, Art. no. 2704.
[5] C. Y.-P. Chao *et al.*, J-EDS, vol. 7, pp. 227–238, 2019.
[6] S.-F. Yeh *et al.*, IISW 2019 (this proceeding).